

Long-Term Load-Deformation Behavior and  
Strength of Elastomer-Based Adhesives

Forest Products Lab.  
Madison, WI

Prepared for

Department of Housing and Urban Development  
Washington, DC

Apr 79

DISTRIBUTION STATEMENT A

Approved for public release;  
Distribution Unlimited

19960223 106

U.S. Department of Commerce

National Technical Information Service

**NTIS.**

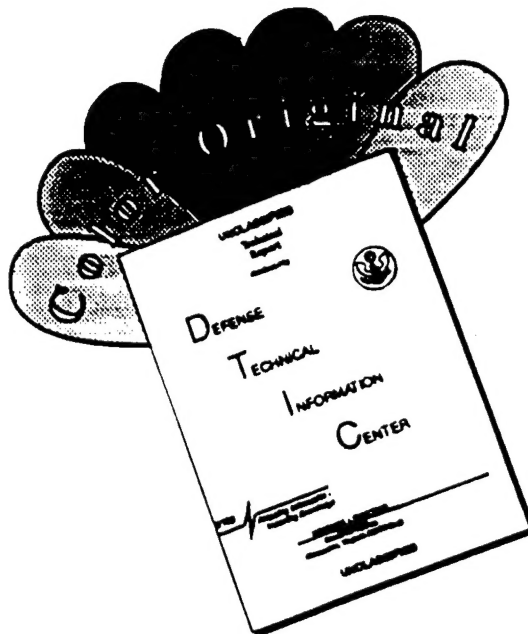
DEPARTMENT OF DEFENSE

PLASTICS TECHNICAL EVALUATION CENTER  
RADCOM, DODFIR, N. J. 07043

DTIC QUALITY INSPECTED 8

4331

# DISCLAIMER NOTICE



THIS DOCUMENT IS BEST  
QUALITY AVAILABLE. THE COPY  
FURNISHED TO DTIC CONTAINED  
A SIGNIFICANT NUMBER OF  
COLOR PAGES WHICH DO NOT  
REPRODUCE LEGIBLY ON BLACK  
AND WHITE MICROFICHE.

HUD-0002226

PB82-175530

---

# LONG-TERM LOAD- DEFORMATION BEHAVIOR AND STRENGTH OF ELASTOMER-BASED ADHESIVES

---

By  
BRYAN H. RIVER, Technologist  
and  
ROBERT H. GILLESPIE, Chemist

April 1979

Forest Products Laboratory  
Forest Service  
U.S. Department of Agriculture  
Madison, Wis.

Prepared for  
Department of Housing and Urban Development,  
Office of Policy Development and Research

REPRODUCED BY  
**NATIONAL TECHNICAL  
INFORMATION SERVICE**  
U.S. DEPARTMENT OF COMMERCE  
SPRINGFIELD, VA 22161

## ABSTRACT

Many new adhesives with promising capabilities for use in building construction have time-dependent mechanical properties. Their use has been limited primarily to nonstructural uses due to lack of knowledge about these properties. This study involved developing a useful test method to evaluate the long-term strength and stiffness of flexible adhesives, and exploring some methods of evaluating adhesive time dependency.

A versatile test apparatus was developed for this purpose, capable of producing creep, stress relaxation, and creep-rupture strength data. A feature of the apparatus is automated collection of data at selected intervals in a format for computer processing. Strain-time data from preliminary tests of five adhesives were analyzed for fit to algebraic expression, creep modulus versus time, isochronous stress-strain behavior, and creep-rupture strength. Problems encountered particularly in the equipment development stages are described and suggestions made for future improvements. In spite of the experimental difficulties, useful data were collected and are presented in a format useful to designers of structures that use flexible adhesives in structural joints.

## BIBLIOGRAPHIC INFORMATION

PB82-175530

Long-Term Load-Deformation Behavior and Strength of Elastomer-Based Adhesives,

Apr 79

Bryan H. River, and Robert H. Gillespie.

PERFORMER: Forest Products Lab., Madison, WI.

SPONSOR: Department of Housing and Urban Development,  
Washington, DC. Office of Policy Development and  
Research.  
HUD0002226

A test apparatus was developed to evaluate the long - term stress - strain behavior of relatively flexible adhesives. The apparatus was designed for use in creep and creep - rupture testing and to be easily convertible to stress - relaxation testing. Information useful to design engineers and adhesive formulators can be obtained with this apparatus. Preliminary tests revealed relationships between adhesive creep modulus and time, evidence of a yield point through isochronous stress - strain curves, trends in recovery behavior, and the creep - rupture strength of several mastic construction adhesives and a two - part polyurethane adhesive. Not all the data obtained were useful. Many problems arose with failure of the electronic data collection system in the development stage. These failures were mainly related to manufacturing defects, however. The slip gage device should be redesigned to compensate for unwanted adherend movement or deformation. The data collection and temperature control systems, while operating satisfactorily, could be improved. These and other p, ....

Available from the National Technical Information Service,  
Springfield, Va. 22161

PRICE CODE: PC A03/MF A01

## TABLE OF CONTENTS

	<u>Page</u>
INTRODUCTION . . . . .	1
Need . . . . .	1
Objective . . . . .	1
Scope . . . . .	2
Terminology . . . . .	2
EQUIPMENT DEVELOPMENT . . . . .	4
Creep Test Chamber . . . . .	4
Slip Gage . . . . .	10
Load Cells . . . . .	12
Data Collection . . . . .	12
Calculation of Corrected Creep Shear Slip . . . . .	16
EXPERIMENTAL . . . . .	19
Adhesives . . . . .	19
Test Specimen . . . . .	19
Loading Procedure . . . . .	21
Test Environment . . . . .	21
Data Processing . . . . .	21
Calculations . . . . .	22
METHODS OF ANALYSIS AND RESULTS . . . . .	23
Curve Fitting . . . . .	23
Creep Modulus . . . . .	25
Isochronous Stress-Strain . . . . .	30
Recovery Behavior . . . . .	32
Creep-Rupture Strength . . . . .	32
Suggested Test Program . . . . .	34
SUMMARY . . . . .	36
BIBLIOGRAPHY . . . . .	37
APPENDIX A . . . . .	39
APPENDIX B . . . . .	41

This work was prepared  
for the

DEPARTMENT OF  
HOUSING and URBAN DEVELOPMENT

Office of  
Policy Development and Research

LONG-TERM LOAD-DEFORMATION BEHAVIOR AND STRENGTH  
OF ELASTOMER-BASED ADHESIVES

By

BRYAN H. RIVER, Technologist  
and  
ROBERT H. GILLESPIE, Chemist

Forest Products Laboratory,<sup>1/</sup> Forest Service  
U.S. Department of Agriculture

INTRODUCTION

Need

Many new adhesives with promising capabilities for use in building construction have mechanical properties that depend upon the time the adhesive-bonded material is loaded. Use of adhesives with time-dependent properties has been limited primarily to nonstructural purposes or those requiring only short-term stiffness, not long-term stiffness or strength. Other materials with time-dependent properties have been used successfully where long-term strength and stiffness are important, e.g., wood beams, plastic water supply pipe, and rubber engine mountings.

New design methods for composite wood structures, such as floor diaphragms (4,8),<sup>2/</sup> wall shear panels (11), and beams (6), have been developed to make use of adhesives less stiff and less strong than wood. But for these applications, long-term strength and long-term stiffness properties must be evaluated and presented to the designer in meaningful terms. This concept of using flexible adhesives with time-dependent properties in building construction was discussed in a previous report (14).

Objective

This study is concerned with the need to develop a useful test method to evaluate the long-term stiffness and strength of adhesives with time-dependent qualities. At the present time there is no standard method for measuring or describing these properties of adhesives. This report may provide a start toward that end, for the increased use of adhesives in building construction promises improved efficiency of wood use and building quality.

---

<sup>1/</sup> Maintained at Madison, Wis., in cooperation with the University of Wisconsin.

<sup>2/</sup> Underlined numbers in parentheses refer to items listed in the Bibliography at the end of the report.

## Scope

The method described here is useful for measuring the long-term load-slip behavior (creep modulus), recovery, or stress-rupture time of thick adhesive layers less stiff and strong than the wood that is bonded. The equipment is relatively simple and yet capable of yielding test results from specimens exposed to temperatures as high as 70° C (160° F) and water soaking. With simple modifications, the apparatus can be converted from constant stress configuration to constant strain configuration, with continual automated monitoring of strain or stress with time.

## Terminology

Load.--The force applied to the specimen at any given time. In creep testing, the load is a constant or dead load.

Slip.--The relative collinear displacement of the adherends on either side of the adhesive layer in the direction of the applied load.

The following definitions of terms used in this report are adopted or adapted from ASTM D-2990 (1) and ASTM E-6 (2):

Shear stress.--The stress component tangential to the plane on which the forces act.

Creep strain.--The total strain at any given time produced by the applied stress during a creep test. Note: The term "creep," as defined in ASTM E-6 and as generally used in rheology, is the nonelastic portion of strain. In actual practice, however, it is difficult to separate the elastic and nonelastic portions of strain of most flexible adhesives. Therefore, such a definition is not practical in the measurement of creep behavior or in applying the measurements to engineering design. The definition provided in ASTM D-2990 reflects current plastics engineering usage and will be used in this report.

Creep recovery.--The total decrease in strain at any given time following the removal of the load.

Creep-rupture strength.--The stress that will cause fracture in a specimen under dead load in a specified time and environment.

Stress-strain diagram.--A diagram in which corresponding values of stress and strain are plotted against each other. Values of stress are usually plotted as ordinates and values of strain as abscissas.

Isochronous stress-strain diagrams.--Log-log plots of the creep strain at a specified time due to each of several levels of constant applied stress.

Creep-rupture envelope.--A stress-time curve of corresponding values of the stress-at-rupture and time-to-rupture plotted against each other.

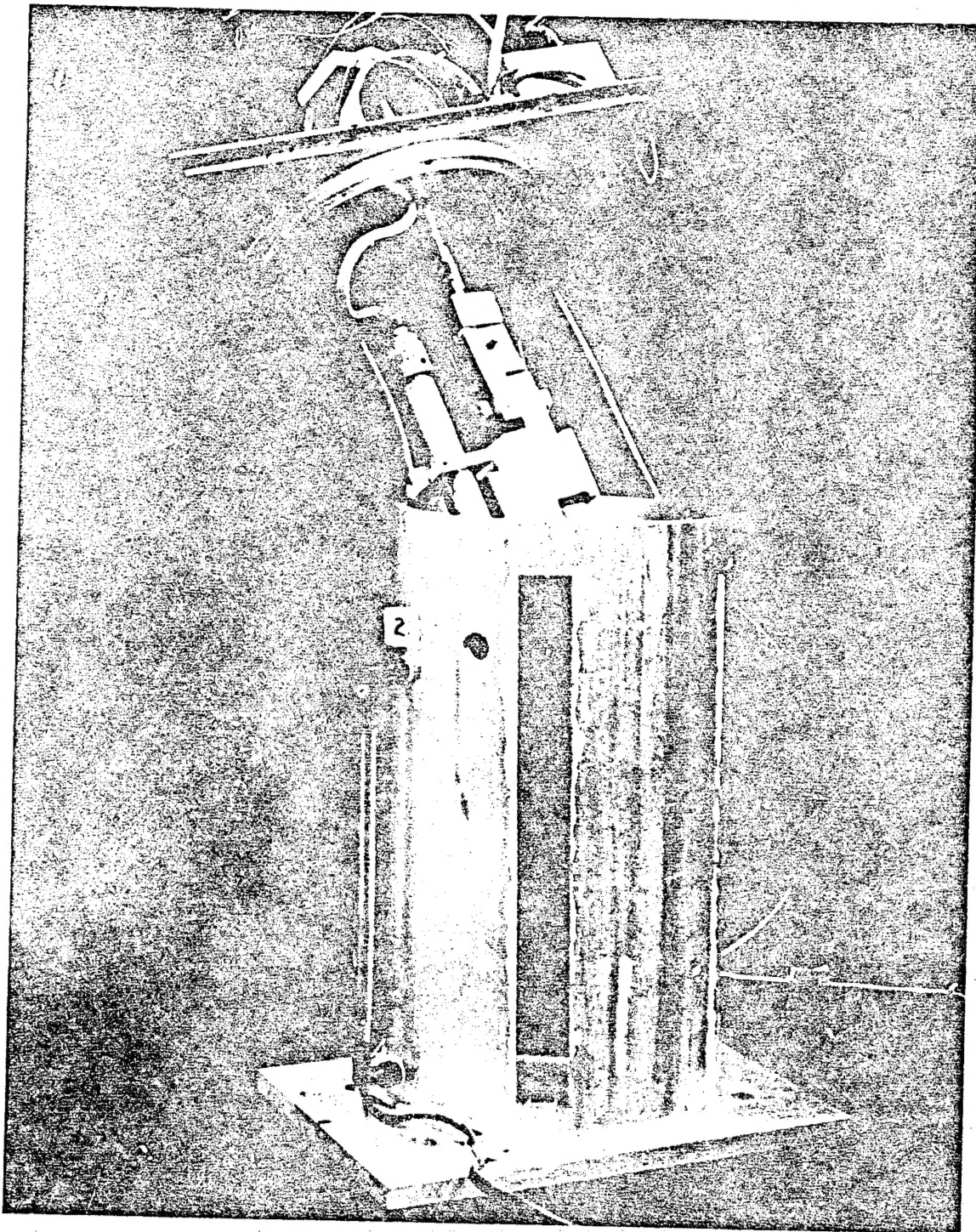


Figure 1.--Individual creep test chamber showing load cell at the top, ports for air movement, sight glass for determining water level, and bonded silicone rubber heating strips.

(M 145 895)

## EQUIPMENT DEVELOPMENT

### Creep Test Chamber

The basic unit of the dead-load test facility is the individual environmental and dead-load chamber. Each chamber supplies relatively constant load, temperature, and moisture to the specimen within it. Loads up to 100 kilograms force (kgf) can be applied directly or up to 1,000 kgf by a lever. Temperature within the chamber can be controlled from ambient room conditions  $23 \pm 1^\circ \text{C}$  ( $74 \pm 2^\circ \text{F}$ ) up to  $70 \pm 0.1^\circ \text{C}$  ( $160 \pm 0.2^\circ \text{F}$ ) using individual heaters and a controller. Moisture condition can be varied from 44% relative humidity (RH) at  $23^\circ \text{C}$  (or ambient at elevated temperatures) to 100% RH or water immersion. In terms of output, each test unit provides continuous readout of the adhesive layer slip, the load, and temperature.

Twenty such chambers, shown in figure 1, were built and installed five to a bench on four benches, as shown in figure 2. Each test unit is constructed of 6-inch Standard 405 type 6061-T6 seamless aluminum pipe, with 1/2-inch-thick aluminum base and top cover plates. The pipe was trued inside and out on a lathe, with a finished inside diameter of approximately 6 inches, and a 11.5-inch-deep cavity for testing. Blueprint drawings of the chamber and support bench are supplied in Appendix A.

#### 1. Load

Test specimens are suspended in the chamber by a rod extending from the top of the load cell ring through the lid to the upper specimen grip (fig. 3). A hardened ground shaft affixed to the lower grip passes through a rubber seal and linear ball bushing assembly and through the bottom of the cylinder. Attached below the hardened shaft is a flexible cable connector which is either fastened directly to the dead load or to a lever by a spherical connector. The rods and grips are made from stainless steel. The remaining components inside each chamber are aluminum. The test units are positioned toward the front of each bench for direct dead loading so the weight pans can be easily handled (fig. 4A). For lever loading, the test units are positioned toward the rear of each bench so the free end of each lever (the end supporting the weight pan) is still located toward the front of each bench (fig. 4B). The lever pivot is fixed but two positions are provided on each lever so that either a 10-to-1, or 20-to-1 ratio of specimen load to actual dead weight can be achieved.

A movable jack platform was constructed to facilitate loading five specimens smoothly and simultaneously. The jack arrangement shown in figure 5 consists of a lower platform on 4-inch hard swivel casters, a 1.5-ton hydraulic jack, and an upper platform to hold the weight pans. The bottom of the jack is welded to the lower platform, while the piston extension fits into a sleeve welded to the underside of the upper platform. Heavy weight pans can be easily loaded in the open onto this jack, then the jack rolled into position under the creep apparatus and raised into position for attachment to the five specimens.

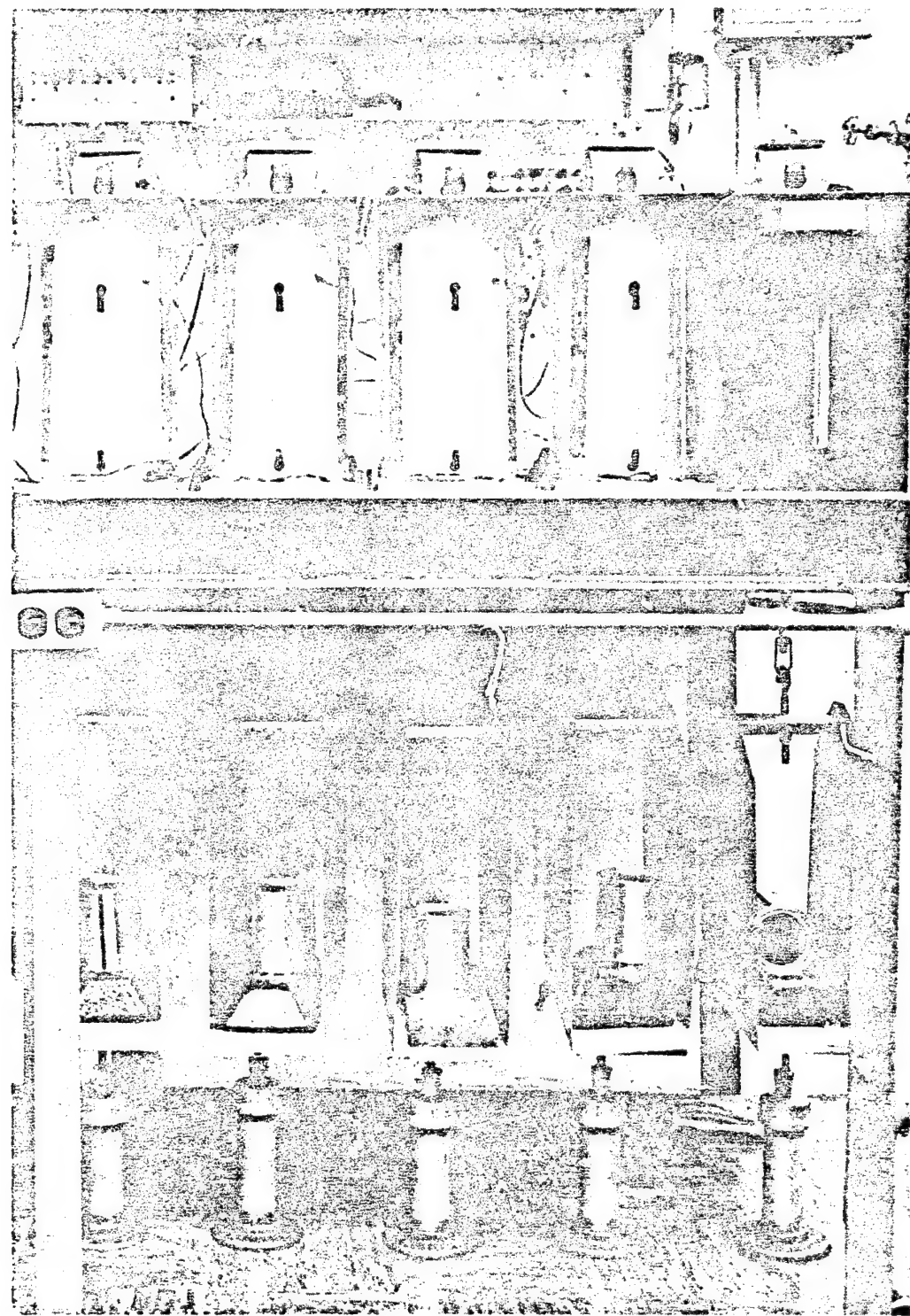


Figure 2.--Five test chambers mounted on a bench capable of supporting their dead load. The chamber at the upper right is enclosed in an individual insulated box for testing at an elevated temperature.  
(M 145 894)

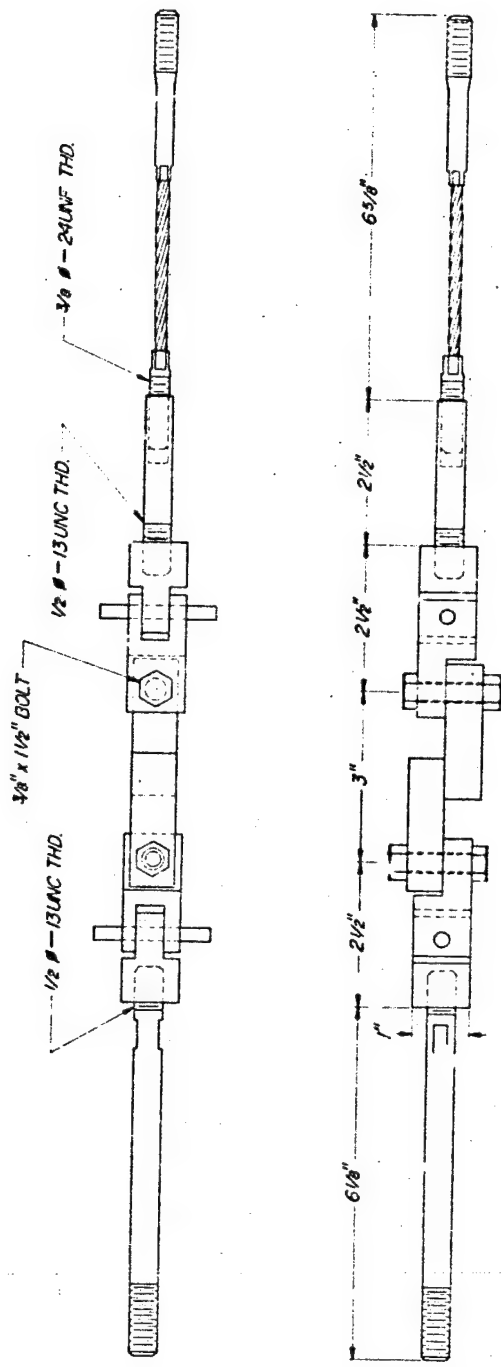


Figure 3.--Side views of loading device. Parts are tension rod (left), upper grip, specimen, lower grip, linear bearing shaft, and cable attachment (right). (M 146 089)

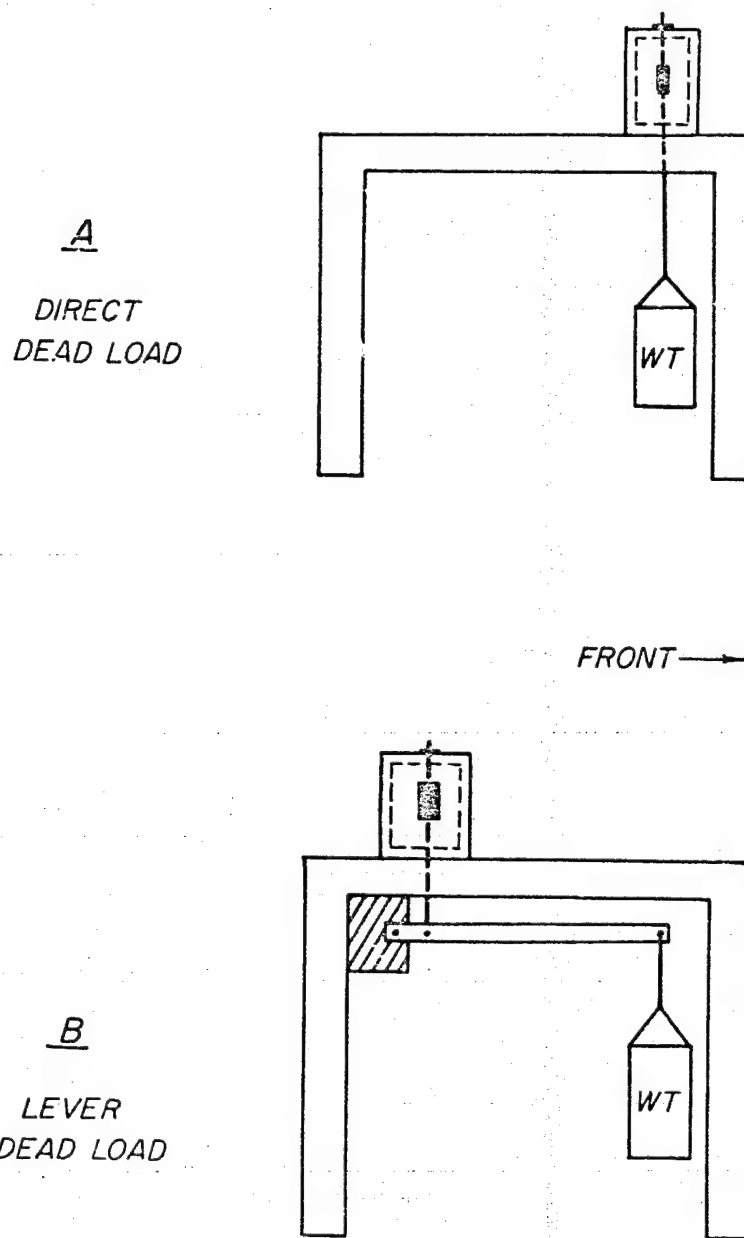


Figure 4.--Schematic drawing of test chamber in: A, the forward (direct dead load) bench position with easy access to the weight pans: B, the rear (lever dead load) bench position maintaining easy access to the weight pans.  
(M 146 257)

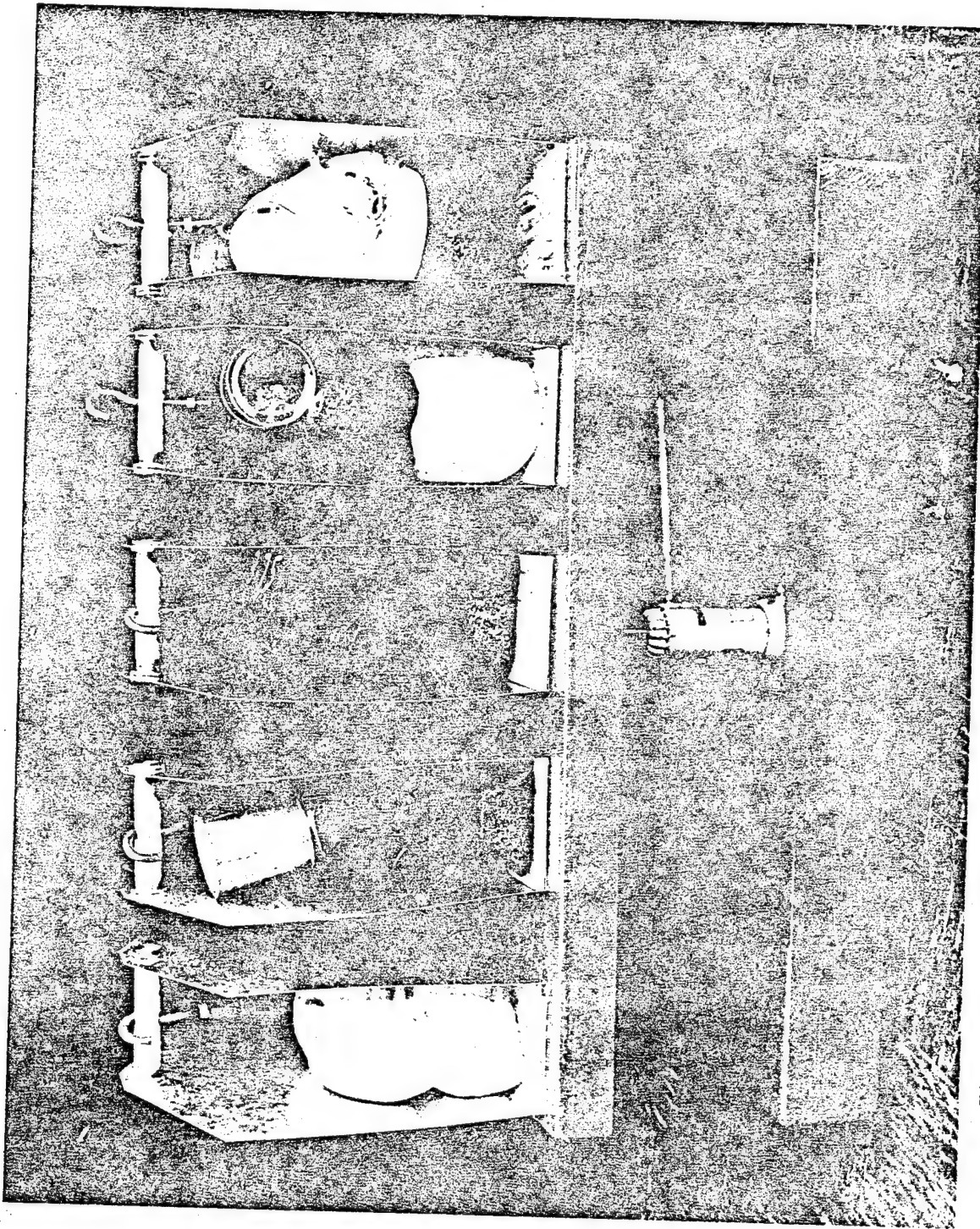


Figure 5.--Hydraulic jack platform for machine

Hydraulic dampers, shown in figure 2, are placed under the weight pans of specimens expected to fail, to reduce shock to adjoining specimens when failure occurs.

## 2. Heat

Heat is supplied by four silicone rubber heating mats bonded to the outside of each cylinder (fig. 1). The heating mats are wired in parallel. The original design called for an individual controller for each chamber. However, as cost mounted, a compromise was necessary. Instead, one controller was used for five chambers, with a variable voltage control between the controller and each chamber to compensate for differences in heat loss among the chambers. A second modification necessitated by this compromise was a common insulated enclosure for the five units instead of five individual insulated enclosures. Each five-unit enclosure was supplied with a fan to help equalize the temperature inside the chambers. (Note: A different heating system from the bonded mats would be preferable when one controller is used for five test units.) But this compromise system worked fairly well, and may in fact be preferable to individually insulated cylinders for replicate testing. By adjusting the voltage supplied to each unit, the temperature spread among the units can be maintained within  $1.0^{\circ}$  C.

The temperature controllers had an accuracy of  $\pm 0.5^{\circ}$  C. Since wood is a good insulator, the  $\pm 0.5^{\circ}$  C temperature variability due to the controllers' on-off cycle is reduced to about  $\pm 0.1^{\circ}$  C at the center of the test specimens. The temperature in each test chamber was read to the nearest  $0.1^{\circ}$  C with a copper-constantan thermocouple and digital temperature indicator. Controller temperature sensing was by a surface thermistor bonded to the wall of the middle test chamber.

## 3. Moisture

Each chamber is supplied with small ports for air to pass through in tests at ambient relative humidity. These ports are closed with a cork during high humidity or water-soak tests. Ambient conditions in the room where the apparatus is located are  $23^{\circ}$  C ( $74^{\circ}$  F) and 44% RH. The ambient relative humidity drops to 9% at  $49^{\circ}$  C ( $120^{\circ}$  F) and 4% at  $70^{\circ}$  C ( $160^{\circ}$  F). These conditions correspond to wood moisture contents of 8, 2, and 1%. They constitute the dry test conditions.

Tests at higher moisture levels were conducted by closing the ports and supplying distilled water to the chamber. Five chambers were hooked to a common supply. The water level in the five chambers was controlled by an adjustable float valve. Each cylinder has a sight glass so the water level can be checked during a test. A pool of water in the bottom of each chamber will result in close to 100% RH at each temperature, depending on how well the cylinders are sealed against vapor loss. These conditions correspond to a wood moisture content of about 28%. They constitute the moist test condition.

Tests of specimens in the water-soaked condition are conducted by raising the float valve assembly until the water level inside the chambers is above the specimen. The rubber seal around the hardened ground stainless steel shaft of the loading apparatus effectively seals the bottom end of the cylinder so the water level can be raised above the well at the bottom. The linear ball bushing restrains the shaft from lateral motion to maintain the seal between the shaft and rubber.

### Slip Gage

Figure 6 shows the aluminum brackets with a linear variable differential transformer (LVDT) comprising the slip gage. One bracket supporting the LVDT is fastened to one adherend and the second bracket, attached to the LVDT core, is fastened to the second adherend. The brackets are attached with screws and the LVDT core is bonded to its bracket with RTV silicone to eliminate unwanted lateral movement.

This slip gage design was the most successful single LVDT gage tested. This gage may yield erroneous measurements if the adherends rotate or bend significantly, or if the wood changes dimensionally during the test. It is possible that a more intricate gage might be designed to eliminate or minimize these effects; however, the precise machining and the quantity required, 20, would have been prohibitive in this exploratory study. The approach to minimize slip gage errors was to:

1. Design each adhesive specimen to eliminate adherend bending.
2. Test each specimen for rotation before accepting it as a creep specimen.
3. Carefully condition each specimen to equilibrium moisture content in its creep test chamber before applying the load.

The procedure for designing joints and a special two-transducer slip gage for measuring rotation are described in a previous report (14). Moisture and temperature equilibrium were assumed when the slip gage LVDT readings remained constant for a period of 24 hours.

### 1. Displacement Transducers

The adhesive shear deformation was measured by the shear displacement or slip of the specimen adherends. The instrument used to measure slip is a linear variable differential transformer (LVDT) manufactured by the SRC Division of Moxon, Inc. The LVDT consists of a sealed body and a movable core. Transducers of two sensitivities were selected: Type I -  $\pm$  5.000 VDC output for  $\pm$  1.27 mm ( $\pm$  0.050 in.) core displacement, and Type II -  $\pm$  5.000 VDC output for  $\pm$  2.54 mm ( $\pm$  0.100 in.) core displacement. Both types have 0.1% linearity. Ten of each type were purchased for the 20 test units. The original equipment design called for all 20 LVDT's to be hermetically sealed for use in high humidity, or immersed in water; however, the cost of hermetically sealed units was twice the standard unit, so only five hermetically sealed LVDT's of each sensitivity were purchased.

Nineteen volts were supplied to the LVDT's in groups of 10 by two identical precision d.c. power supplies. The LVDT input and output voltages were continuously recorded by a data handler and collection system described later.

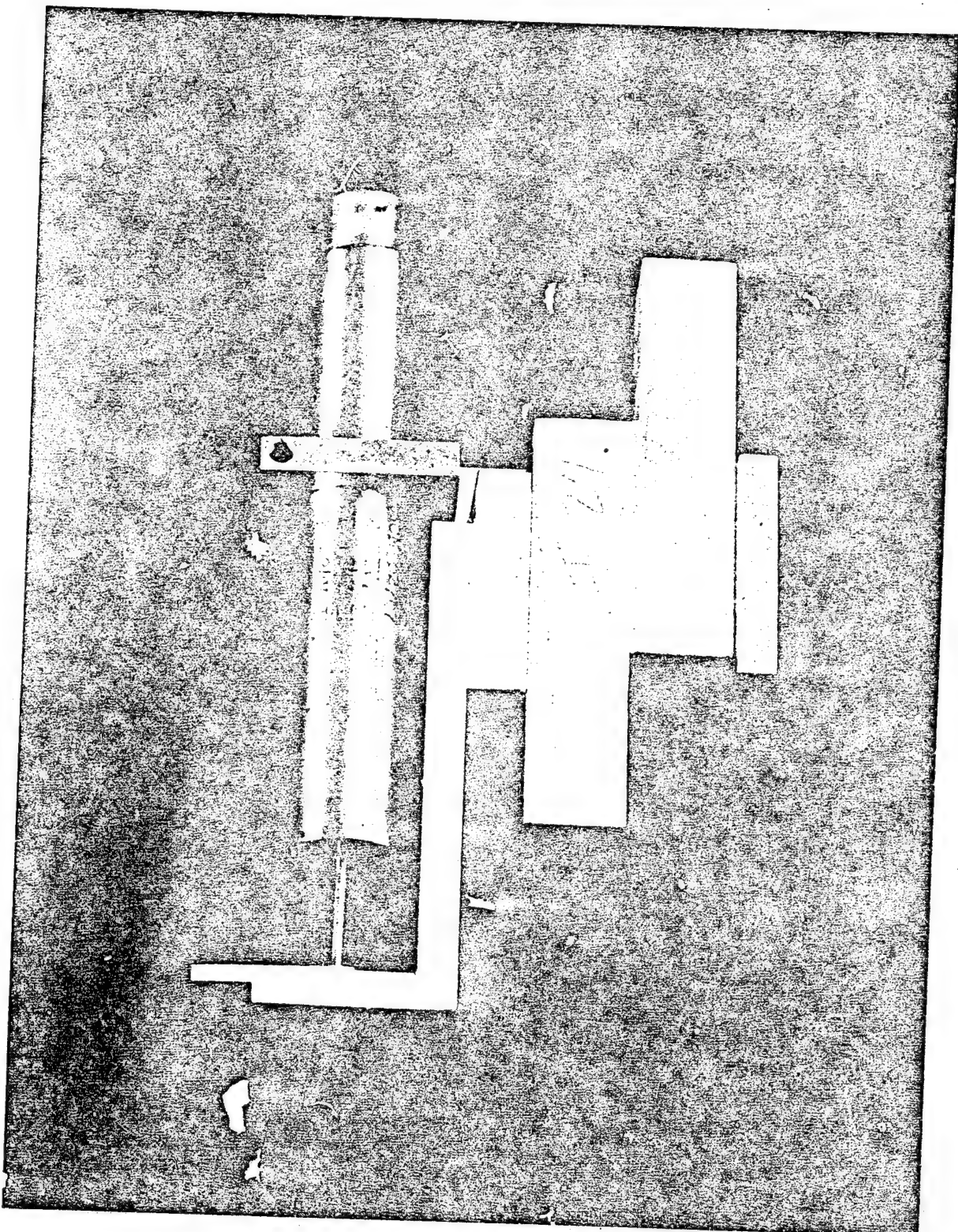


Figure 6.--Aluminum slip gage with LVDT mounted on a thick adherend single-lap shear creep specimen. The bracket supporting the LVDT is fastened to the right adherend and the bracket to which the LVDT core is attached is fastened to the left adherend. (M 145 896)

## 2. LVDT Calibration

Each LVDT was calibrated for voltage output as a function of core displacement and input supply voltage.<sup>3/</sup> Two sets of LVDT output voltage measurements were made at five core positions with a given input voltage. Then the procedure was repeated at four additional voltages. The calibration points were:

### Type I LVDT

Core position	1.0, 0.5, 0, -0.5, -1.0 mm
Input voltage	16, 18, 20, 22, 24 VDC

### Type II LVDT

Core position	2.0, 1.0, 0, -1.0, -2.0 mm
Input voltage	16, 18, 20, 22, 24 VDC

This two-way calibration enabled correction of the LVDT output voltage for any short- or long-term variation in the input voltage. The development of this correction procedure is explained in Appendix B. The final equation for accomplishing the correction is discussed in the section on data correction.

Figures 7 and 8 show the two calibration plots for LVDT output voltage ( $V_o$ ) versus core position ( $\Delta$ ), and output voltage ( $V_o$ ) versus input voltage ( $V_I$ ).

## Load Cells

Load cell rings were machined from type 6061-T6 seamless aluminum pipe. Outside diameter was 2.990 inch. The wall thickness of the rings varied with load capacity, 0.126 inch for 100 kgf rings, and 0.365 inch for 1,000 kgf capacity rings. See Appendix A for more details. Four phenolic-glass-foil transducer-grade strain gages were bonded to the inner and outer walls of each ring, as shown in figure 9, using a special epoxy adhesive for long-term load applications.

The gages were wired to form a Wheatstone bridge with four active arms, as shown in figure 9. The wiring included a zeroing or balancing potentiometer and polarity reversal switch. Load applied to the ring changes the resistance of the gages. The resistance change is additive for maximum output. The resistance change causes a voltage-current change in the direct current output side of the bridge. The voltage change is measured. Most of the load cells produced approximately 0.0160 VDC output under full scale load when supplied with a 10-volt excitation. In conjunction with a voltmeter reading to 0.0001 volt, it is possible to resolve 0.625 and 6.25 kgf with the 100 kgf and 1,000 kgf rings, respectively.

## Data Collection

Data from the displacement transducers is fed to an automatic data acquisition system consisting of a data coupler, analog scanner, digital panel voltmeter, day counter, and digital hours-minutes-seconds clock.

In operation the system records the day and time and then sequentially scans from 1 up to 60 channels of input data. The input data may vary from -4.0000 VDC

<sup>3/</sup> Even though very stable power supplies were used, their output voltage drifts over the long time period of a creep test. After determining the LVDT input-output voltage coefficient, the computer was used to correct each LVDT output reading for power supply drift.

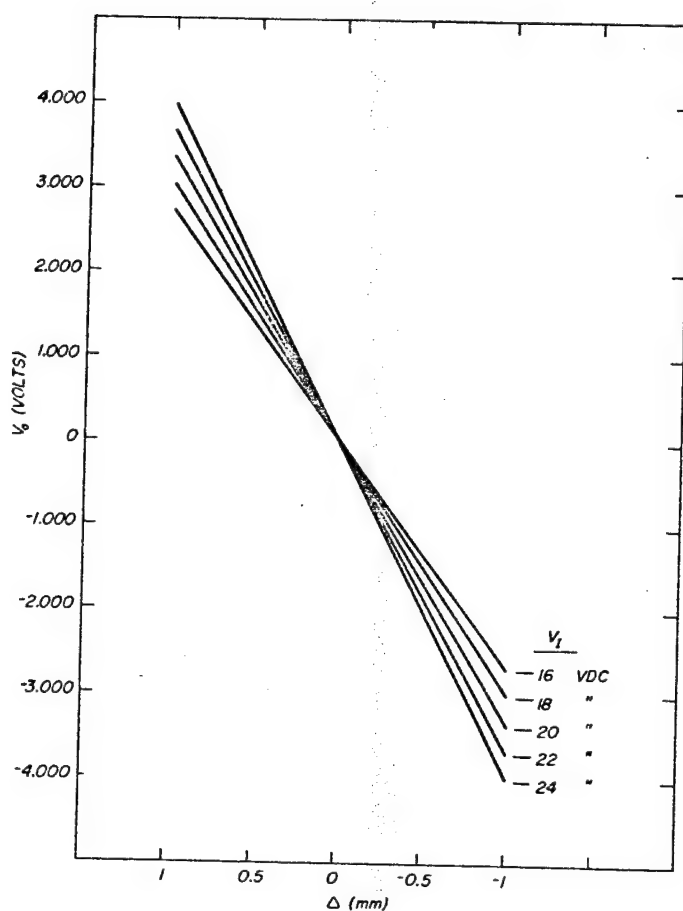


Figure 7.--Sample calibration plot of one LVDT voltage output ( $V_o$ ) as a function of the core position ( $\Delta$ ) and the change in the relationship  $dV_o/d\Delta$  as a function of the input voltage ( $V_I$ ).  
 (M 146 252)

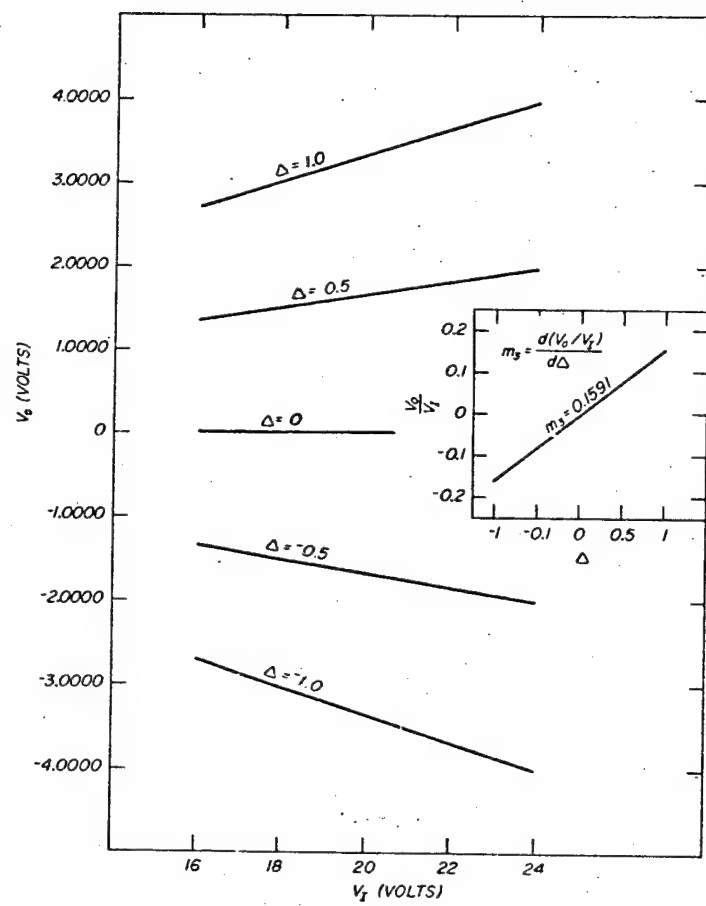
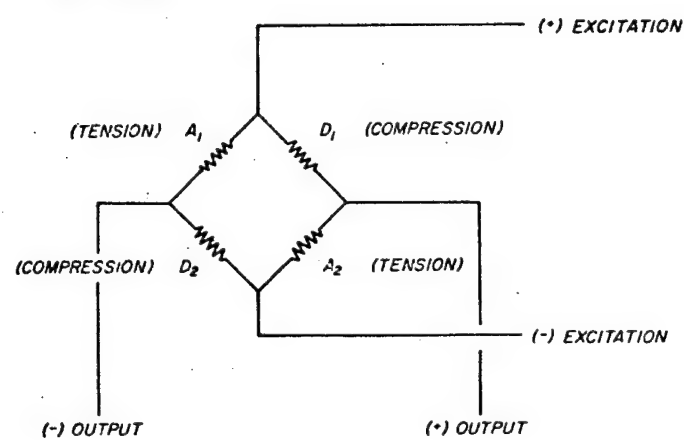


Figure 8.--Sample calibration plot of one LVDT voltage output ( $V_o$ ) as a function of the input voltage ( $V_I$ ) and the change in the relationship  $dV_o/dV_I$  as a function of the core position ( $\Delta$ ).  
(M 146 251)

GAGE WIRING



GAGE LOCATIONS

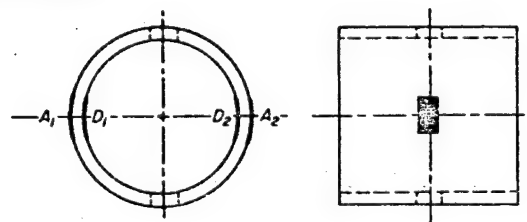


Figure 9.--Strain gage arrangement and wiring diagram for an additive four-arm bridge load cell.  
(M 146 248)

to  $\pm 4.0000$  VDC. The scanner will read 40 channels per minute. The frequency of scan is variable from 1 minute to several days. Digitized data from each channel is then recorded on a teletype. Punched paper tape output is also available for computer processing.

Originally the system was designed to use all 60 channels, recording the LVDT, load cell, and thermocouple outputs of each test unit. For various reasons, this design was not practical. The present system is designed to read the power supply voltage to each LVDT and then the LVDT output for each test unit in turn. This particular change was necessitated by power supply drift over the duration of the creep tests. Recording the input and output voltages in this fashion allows the computer to correct the LVDT output according to its input at a given time by the equation provided in the following section. Figure 10 shows a single teletype recorded scan of 40 channels (20 test units).

For the present work, direct dead loads are used without concern for the possibility of load changing during test, so load cell output is not recorded. Secondly, the thermocouple output would require additional signal amplification to obtain useful resolution with the  $\pm 4.0000$  VDC digit panel meter of the data acquisition system. Continual high resolution temperature sensing and recording would be a useful feature to further improve this system.

Data acquisition systems now available, provide for signal amplification and conversion to engineering units which the present system does not.

#### Calculation of Corrected Creep Shear Slip

In this study the creep shear slip is assumed equal to the LVDT core displacement. The core displacement, in turn, is in proportion to the LVDT voltage output at a given voltage input, as shown in figure 7. Thus:

$$S = \Delta_o - \Delta_t = \frac{V_o - V_t}{b} \quad (1)$$

where:

$S$  = creep shear slip,  
 $\Delta_o - \Delta_t$  = core displacement from start (o) to some time (t),  
 $V_o$  = LVDT voltage output at test initiation,  
 $V_t$  = LVDT voltage output at time (t), and  
 $b$  = regression coefficient from the relationship  $V_o = a + b\Delta$ .

But because the input voltage may vary over the long time of a creep test and the LVDT output voltage is a direct function of the input voltage (i.e.,  $V_o = a + m V_I$ ,  $V_I$  = input voltage) the equation below was developed to calculate the creep shear slip as shown in Appendix B.

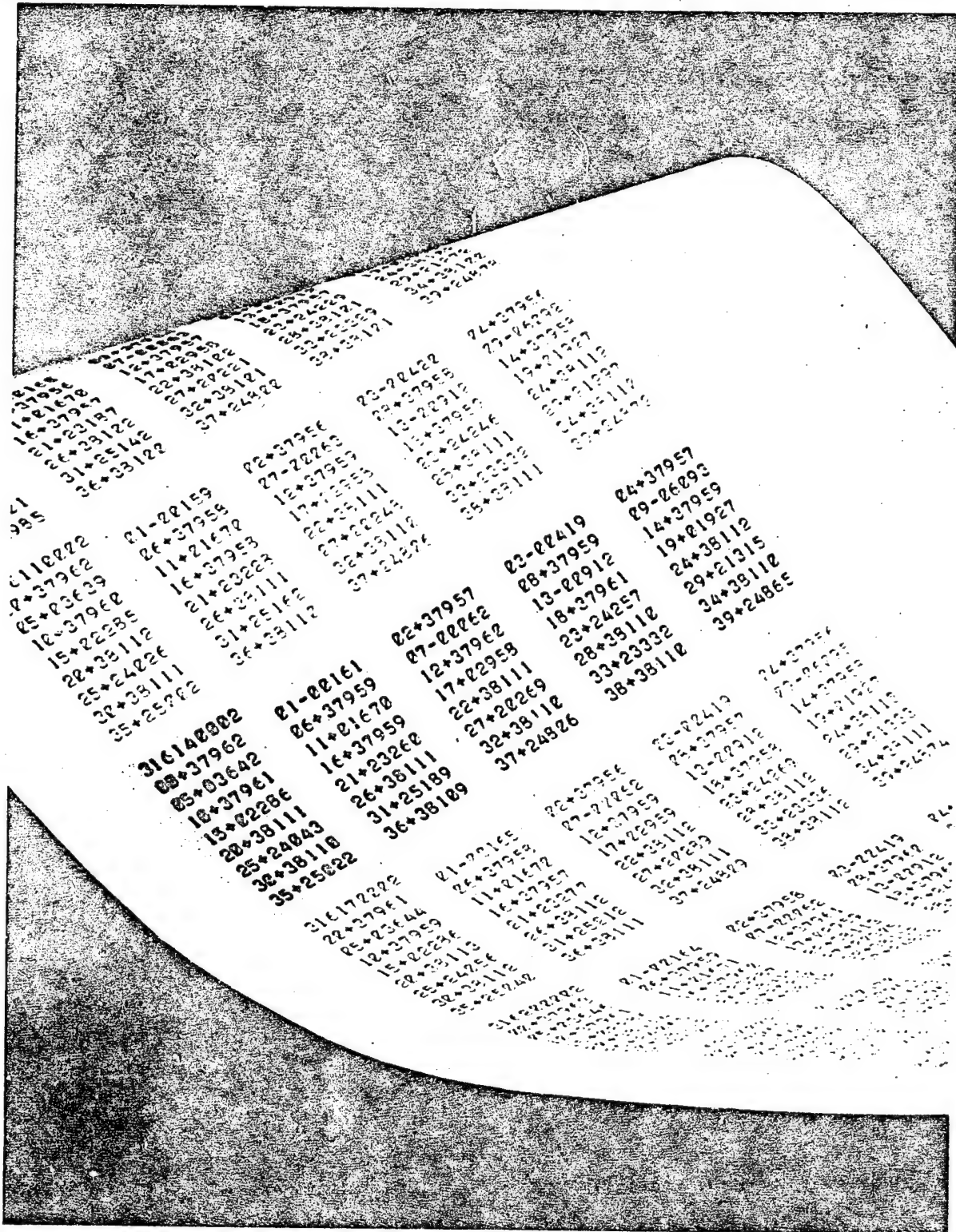


Figure 10.--Teletype record of the time of data collection and the LVDT input and output voltages for 20 test units. The number 316140002 represents the day and time, i.e., 316th day, 14 hours (2:00 p.m.), 00 minutes, and 02 seconds. The first two digits of the remaining numbers indicate the data channel. Odd-numbered channels are LVDT input voltage. The following even channel is the corresponding output voltage. The (+) or (-) signs indicate plus or minus voltage. Numbers following these signs indicate the d.c. voltage.

(M 145 897)

$$S = \Delta_o - \Delta_t = \frac{1}{m} \left( L_o - L_t \right) \quad (2)$$

where:

$$m = \text{LVDT coefficient} \quad \left\{ \begin{array}{l} 0.1600 \text{ for Type I LVDT} \\ 0.0800 \text{ for Type II LVDT} \end{array} \right.$$

$$L_o = \frac{V_{o_o}}{V_{I_o}}$$

$V_{o_o}$  = initial voltage output

$V_{I_o}$  = initial voltage input

$$L_t = \frac{V_{o_t}}{V_{I_t}}$$

$V_{o_t}$  = voltage output at time (t)

$V_{I_t}$  = voltage input at time (t)

## EXPERIMENTAL

### Adhesives

A brief summary of the adhesive's physical, chemical, and mechanical properties is given in table 1.

Adhesives C, A, W, and M are commercially available mastic adhesives commonly used in building construction. Adhesives C, A, and W have been certified to meet or exceed the requirements of the American Plywood Association Specification AFG-01 for use in the Association's glued floor system. Adhesive D is commercially available, and used in industrial applications for bonding and repair of metal, rubber, cloth, wood, and other materials. All of these adhesives form a cross-linked molecular network soon after bonding.

### Test Specimen

The key to accurate measurement of the stress-strain behavior of adhesive layers in single lap joints is to design the joint to minimize stress concentrations within the layer under load. Stress concentrations are less of a problem in long-term tests of viscoelastic adhesives than in short-term tests, since they will be relieved with time. Still, for the most accurate results, particularly in defining the early portions of the creep and recovery curves, stress concentrations should be minimized. This can be done by designing the joint so the stress uniformity parameter  $\frac{\beta_c}{t}$  is less than 1.0 as described in an earlier report (14).

$$\frac{\beta_c}{t} = \sqrt{\frac{8Gt}{\eta E}} \cdot \frac{c}{t} \leq 1.0 \quad (3)$$

where:

$G$  = short-term adhesive shear modulus,  
 $t$  = adherend thickness,  
 $\eta$  = adhesive thickness,  
 $E$  = adherend tensile elastic modulus, and  
 $c$  = 1/2 the joint overlap length.

The earlier report describes a tension lap shear specimen with standardized hard maple (*Acer saccharum*, Marsh) adherends. The standard adherend is 20 mm wide, 16 mm thick, and must have a specific gravity of not less than 0.65. The tensile elastic modulus of maple at a specific gravity of 0.65 is approximately 12,600 MPa. With adherend thickness ( $t$ ) and modulus ( $E$ ) fixed and an estimate of the adhesive shear modulus, the joint overlap length and, if need be, the adhesive layer thickness can be manipulated to produce a test specimen with the desired  $\frac{\beta_c}{t}$  value.

Table 1.--Some properties of elastomer-based adhesives used in this study

Adhesive designation	Elastomer	Liquid vehicle	Solids	Shear modulus <sup>1/</sup>	Shear strength <sup>2/</sup>
C	Neoprene-phenolic	Petroleum distillate, acetone, toluene	53	35	8.4
A	Polyurethane (1-part)	None	99	1.01	2.42
D	Polyurethane (2-part)	None	99	15.9	2.90
W	Acrylic latex	Water	40	1.34	3.10
M	Polyurethane (1-part)	None	99	2.79	3.33

<sup>1/</sup> Short-term shear modulus measured at 23° C-44% relative humidity under a 0.20 MPa cyclic stress (0.0667 Herz).

<sup>2/</sup> Strength measured at 23° C-44% relative humidity.

In this study specimens for adhesives listed in table 1 had average adhesive layer thicknesses as follows: Adhesive C - 0.5 mm, A - 0.5 mm, D - 0.6 mm, W - 0.5 mm, and adhesive M - 0.9 mm. Joint overlap lengths of 20, 50, 20, 50, and 50 mm, respectively, satisfied the requirement for  $\frac{BC}{E}$  less than 1.0 in each case.

A jig described in the earlier report (14) was used to control adhesive layer thickness. All specimens were bonded initially with a 50-mm overlap length. When necessary the lap length is shortened by sawing equal amounts from the free end of both adherends.

#### Loading Procedure

The specimen with slip gage in place and grips and tension rods attached is placed in the test cylinder. The upper tension rod passes through the cylinder cover and the load cell, and is fastened by a nut on top of the load cell. The LVDT is adjusted manually to a core position near the maximum retracted position and then the cylinder cover is closed. The initial voltage output of the LVDT is recorded, then checked periodically for 24 hours or until there is no further change. This is best done by using the automatic data collection system.

The weight pans are prepared during the period required for the LVDT to reach an equilibrium reading. Five weight pans are placed on the jack and then positioned under the test chambers for attachment to the lower tension cable. Attachment should be made very carefully without disturbing the specimen. Several LVDT readings 2 to 3 minutes apart will reveal if the LVDT is still at equilibrium.

In the present test setup, the data handler scans 40 channels per minute. It thus requires 15 seconds to scan a replicate of five specimens (2 channels per specimen) so there is a slight error built into the early creep strain readings. Using the jack, each set of five specimens is loaded 15 seconds before the first specimen in the set is scanned. Thus the first specimen is read 15 seconds after loading and the fifth specimen is read 30 seconds after loading. The hydraulic jack platform allows the load to be applied smoothly in 1 to 5 seconds.

#### Test Environment

The data described in the Results were obtained from specimens exposed at 23° C and 44% relative humidity.

#### Data Processing

In the early period after loading, readings are made every 2 minutes. After about 10 minutes, the scan frequency is decreased to 5 or 10 minutes and after 4 to 8 hours, the scan frequency is changed to 30 minutes. Finally after 24 hours the frequency is reduced to once every hour.

The large volume of data collected is processed by computer in three steps: (1) Error search and edit. (2) Convert LVDT output voltages to adhesive strains, arrange data according to replicates at like conditions, and attach an identifier. (3) Convert date-time of each strain to minutes. Optional steps may include averaging strains, plotting individual or average strains versus time, and fitting an equation to the data or various calculations of time-dependent behavior based on the data.

Calculations

$$\frac{\text{Dead load}}{\text{shear stress}} = \frac{\text{Load}}{\text{Bond area}} \quad (4)$$

$$\frac{\text{Creep rupture}}{\text{stress}} = \frac{\text{Load}}{\text{Bond area}} \quad (5)$$

$$\text{Creep modulus} = \frac{\text{Load}}{\text{Bond area}} \times \frac{\text{Adhesive layer thickness}}{\text{Creep shear slip}} \quad (6)$$

$$\text{Fractional recovery} = 1 - \frac{\text{Unrecovered strain}}{\text{Maximum creep strain}} \quad (7)$$

$$\text{Reduced time} = \frac{\text{Recovery time}}{\text{Preceding creep time}} \quad (8)$$

## METHODS OF ANALYSIS AND RESULTS

A tracing of a direct computer plot of the creep strain and recovery versus time is shown in figure 11. The shape of the creep and recovery curves shown is characteristic of the behavior of adhesive's C, D, and W. Adhesive A had a greater instantaneous elastic strain upon loading and instantaneous recovery upon unloading. Adhesive A's creep and recovery were less time dependent than the other adhesives.

### Curve Fitting

Since it is not feasible to conduct creep tests for time periods equal to the service life of a structure, it is useful to fit an equation to the data for extrapolating creep behavior beyond economically feasible test periods.

Attempts to fit equations to this creep data were moderately successful using the power law, a common expression for creep behavior, as the starting point.

$$\epsilon(s) = As^p \quad (9)$$

Where

$\epsilon(s)$  = time-dependent shear slip,  
A = nonlinear material function of stress,  
s = time, and  
p = material function.

This equation was fitted in two linearized forms:

$$\log_e y = \log_e a + b \log_e x \quad (10)$$

and

$$\log_e y = \log_e a + b \log_e x + \frac{c}{xm} \quad (11)$$

where

y = time-dependent shear slip,  
a, b, and c = derived material constants,  
x = time in minutes, and  
m = selected exponent.

These equations were fit to sets of data for adhesives A and D in two segments--one corresponding to the creep portion and the other to recovery. Each set was comprised of five specimens. For adhesive D, the starting point for the creep

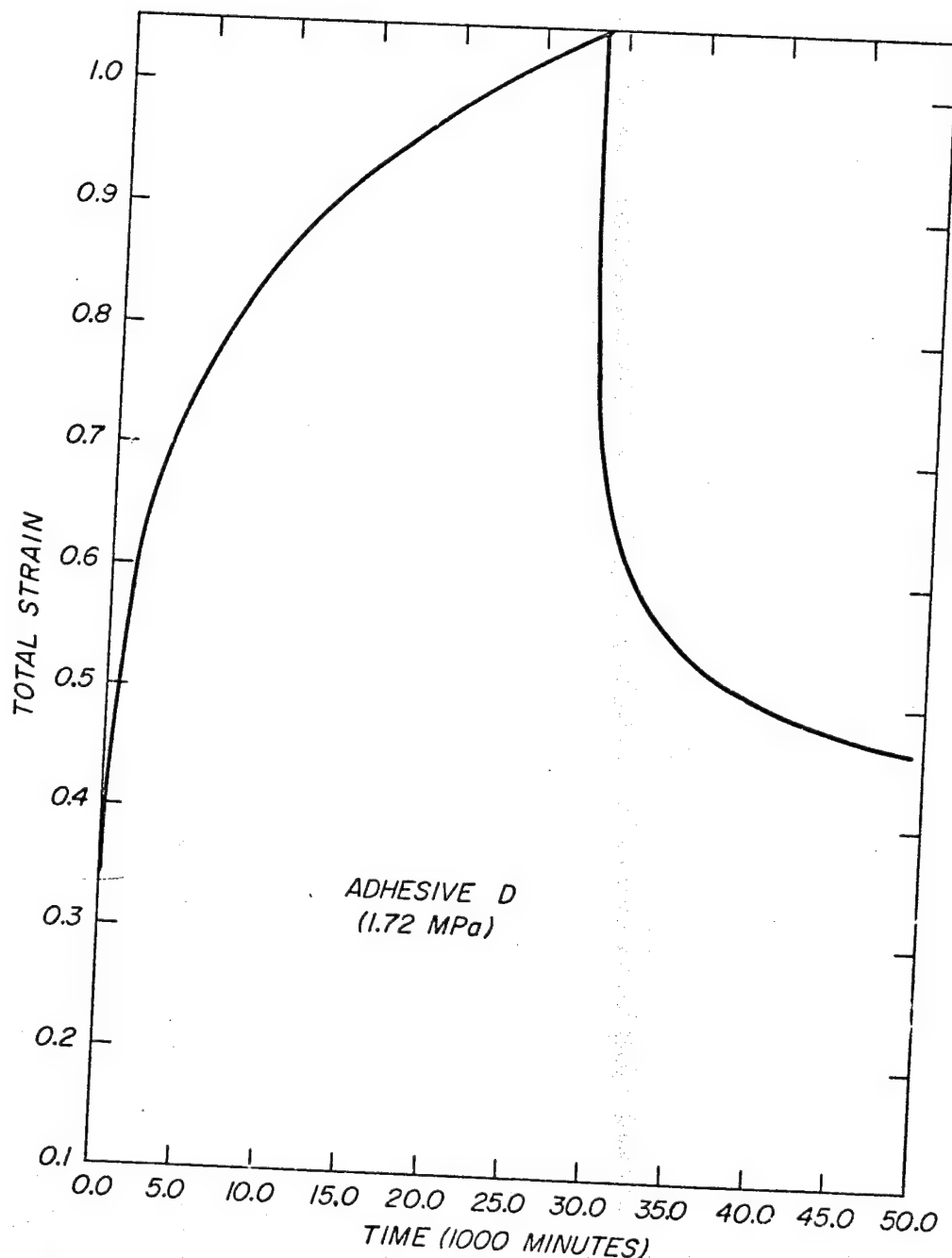


Figure 11.--Direct computer plot of the total creep strain versus time after editing and transformation of the voltage to strain and date-time to minutes. (M 146 256)

equation was zero strain, and for the recovery equation the starting point was the maximum creep strain. Adhesive A had large instantaneous elastic strain upon loading or removal of load. This instantaneous strain amounted to approximately 0.3380 mm/mm upon loading and 0.3580 mm/mm upon unloading. For curve fitting then, the starting point for the creep equation was 0.3380; for the recovery equation, it was the maximum creep strain minus 0.3580. For plotting, the instantaneous strain must be added to the equation result. The fitted equations are shown in table 2. Three equations include the term  $1/x^7$ , found to improve the fit in the rapidly changing early portions of the curve. Figure 12 shows tracings of the actual curve and the fitted curve for adhesive D at 0.74 MPa constant stress. The fit of adhesive A was as good, while adhesive D at 0.49 MPa constant stress had considerable deviations in the creep curve.

#### Creep Modulus

In the absence of an adequate, simple theory to explain the stress-strain behavior of nonlinear viscoelastic adhesives, the plastics industry has adopted the concept of creep modulus (3,5). Creep modulus is calculated the same as the elastic shear modulus (see equation (6)) except that the strain is time-dependent. For this reason creep modulus must be identified by time, but this should not present a problem to designers. Wood structure designers currently apply design factors for duration of load (9). The designer concerned with a snow load, for example, may choose a creep modulus at 1 month. This, of course, is a simplification since creep modulus must also be related to temperature, moisture, and possibly fabrication variables.

Plots of creep modulus versus time not only provide values for use in conventional design equations but also a realistic rank of materials. The behaviors of five adhesives from this study are compared in figure 13. In the figure, creep modulus is plotted versus time for convenience. Adhesive M's behavior appears to be linearized by the semilog relationship:  $G_t = 1/B (\log x - A)$ . The behavior of the other adhesives is not linearized by the semilog transformation, but fit the logarithmic-hyperbolic relationship used by Kinney (5):

$$G_t = \frac{A + B \log x}{1 + C \log x} \quad (12)$$

where

$G_t$  = creep modulus,

A, B, C = regression coefficients, and  
 $x$  = time in minutes.

Fitted coefficients for the equation, based on five specimens of each adhesive, are shown in table 3. Adhesives D and M had four equations. The coefficients for adhesive M are uniform from equation to equation; adhesive D's coefficients are quite variable and the reason for the variation is not apparent. The agreement between the observed and predicted values was excellent in all cases. The greatest difference was 0.06 MPa but, in most cases, their difference ranged from 0 to 0.02 MPa.

• Table 2.--Fitted creep and recovery equations

Adhesive	Stress level	Equations
<u>MPa</u>		
A	0.2	Creep $y = e^{(-2.8879 + 0.1625 \log_e x)} + \gamma_1$ Recovery $y = e^{(-2.3207 + 0.699 \log_e x)} + \gamma_2$
D	0.3	Creep $y = e^{(-3.8775 + 0.2988 \log_e x)}$ Recovery $y = e^{(-1.279 - 0.0321 \log_e x + (0.10328)^{32} \div x^7)}$
D	0.2	Creep $y = e^{(-4.0598 + 0.2230 \log_e x + (0.26744)^{27} \div x^7)}$ Recovery $y = e^{(-0.7394 - 0.1755 \log_e x + (0.10121)^{32} \div x^7)}$

1/  $\gamma$  = instantaneous elastic strain upon loading = 0.3380.

2/  $\gamma$  = instantaneous elastic recovery upon unloading = 0.3580.

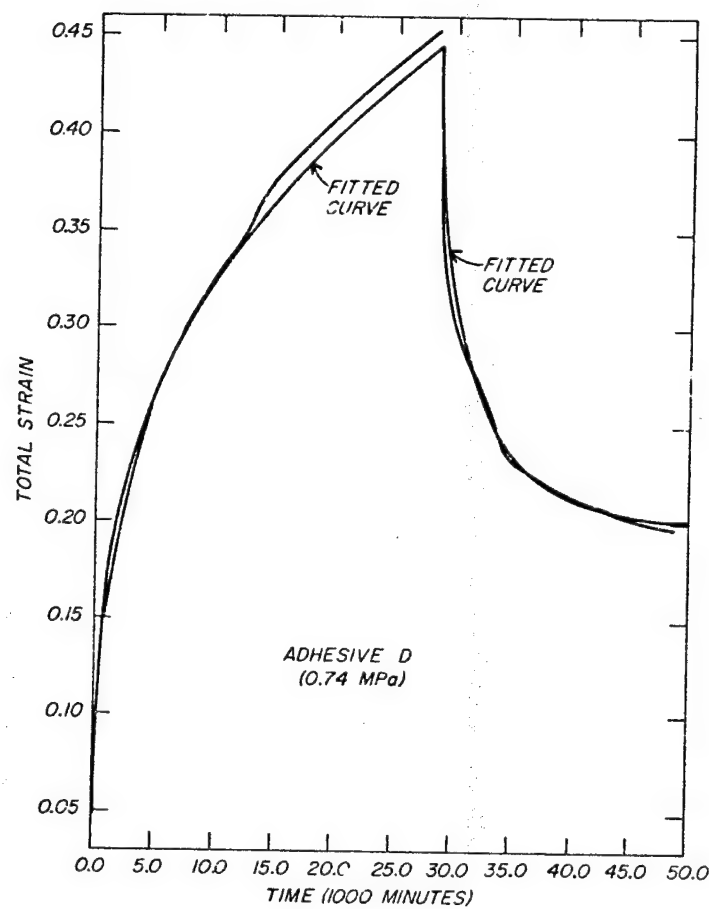


Figure 12.--Observed creep strain versus time curve for adhesive D and a curve corresponding to the fitted equations for creep and recovery.  
(M 146 255)

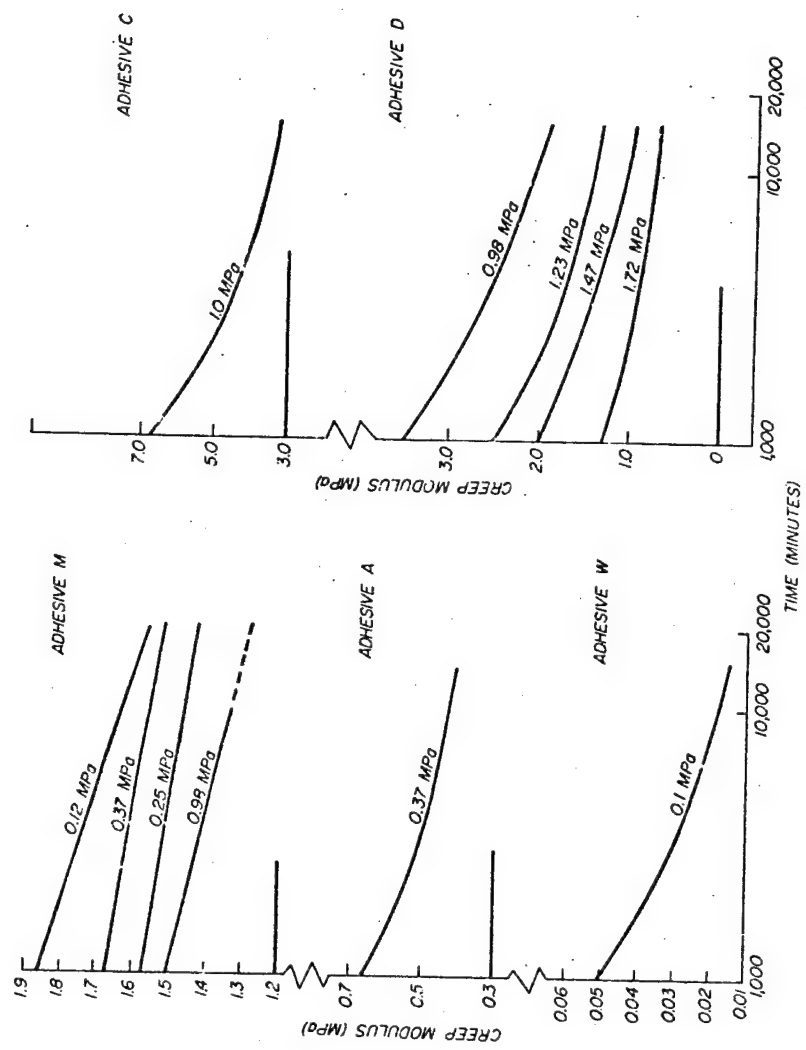


Figure 13.--Creep modulus versus time for adhesives tested at 24° C and 44 percent relative humidity.  
(M 146 254)

Table 3.--Coefficients for logarithmic-hyperbola<sup>1/</sup> fitted to the creep modulus versus time data of several flexible adhesives

Adhesive	Stress level	A	B	C
MPa				
A	0.37	-0.1245	-0.0869	-0.5274
C	1.00	-3.5789	-0.0460	-0.5189
D	0.98 1.23 1.47 1.72	-17.5030 4.9080 -19.1167 -2.4096	1.8194 -0.8356 2.7889 0.2067	-1.4892 0.0223 -2.1236 -0.7935
M	0.12 0.37 0.25 0.98	2.4945 1.8546 1.9224 1.9417	-0.2478 -0.1227 -0.1698 -0.1963	-0.0194 -0.0198 -0.0511 -0.0326
W	0.10	-0.1184	0.0218	-0.6806

1/ Equation (12).

Table 4.--Predicted creep modulus<sup>1/</sup> of several flexible adhesives

Adhesive	Stress	Creep modulus			
		1 week	2 months	10 years	50 years
	MPa	MPa	MPa	MPa	MPa
A	0.37	0.43	0.34	0.28	0.25
C	1.00	3.50	2.39	1.56	1.18
D	0.98 1.23 1.47 1.72	2.06 1.44 1.06 0.73	1.30 0.65 0.54 0.46	0.59 -0.62 <sup>2/</sup> 0.03 0.23	0.19 -1.79 <sup>2/</sup> -0.26 <sup>2/</sup> 0.18
M	0.12 0.25 0.37 0.98	1.63 1.48 1.56 1.33	1.39 1.38 1.44 1.15	0.95 1.19 1.19 0.80	0.48 0.99 0.86 0.40
W	0.10	0.018	0.004	-0.008 <sup>2/</sup>	-0.014 <sup>2/</sup>

1/ Based on behavior observed for 1-1/2 to 3 week periods.

2/ Values less than zero are indicative of failure.

Table 4 is an example of how creep modulus versus time data might be presented for use by a designer selecting an adhesive for a structural application. In most cases, these long-term moduli are in the range of shear modulus values obtained from short-term testing at low stress levels but elevated temperature, or from testing to failure at ambient temperature, as reported in a previous study (13).

#### Isochronous Stress-Strain

The isochronous stress-strain diagram, as defined in the Terminology, is a plot of the creep-strain value attained after a specific time under a constant stress. The diagram may be generated by extracting creep-strains at the specified time from a series of long-term creep curves at different stress levels. Alternatively, the diagram may be generated from a single specimen in a series of short-term creep and recovery experiments, as described by Turner (16). The experiment entails loading the specimen to a low stress level in a universal testing machine, holding that level for the specified time, and then releasing the load, allowing the specimen to recover. After a recovery period equal to four times the load time, the specimen is loaded to a higher stress level. The experiment is repeated at increasing stress levels until enough points are available to plot the curve.

The short-term isochronous stress-strain experiment can be useful in several ways: (1) An initial isochronous experiment can be used to select useful stress levels for the long-term creep experiments. (2) The curve may reveal a yield point of the adhesive at some stress. (3) It is a useful test for quickly ranking adhesives for creep resistance in a specified environment. (4) Isochronous experiments can be used to check the accuracy of long-term creep experiments. (Possibly the most valuable use of isochronous data is to reduce the number of long-term creep experiments needed to define an adhesive's viscoelastic response.) (5) Isochronous curves at 2 or 3 time periods can be used to interpolate between creep curves.

Figure 14 presents examples of isochronous stress-strain curves for four adhesives at 23° C obtained by applying a constant stress at several levels for 6 minutes each level, and 24 minutes recovery between stress application. Each curve represents the average of five specimens. The yield points of each adhesive, where the log-log plot changes from linear to curvilinear, is indicated for each adhesive.

Data from the present study illustrates points 2, 3, and 4 above. The indicated yield point for adhesive W is 0.2 MPa. In the long-term dead loading experiment, all the specimens loaded to a stress of 0.2 MPa, or greater, failed. The indicated yield point for adhesive D was 1.0 MPa. Adhesive D had numerous failures above 1.0 MPa stress level in the long-term experiment and none below.

Attempts to check the validity and accuracy of the long-term experiment were not successful due to specimen variability and because different specimens were used for the short-term isochronous experiment and for long-term creep. Short-term isochronous data should be obtained from the actual creep specimens before the creep experiment to check the creep data accuracy.

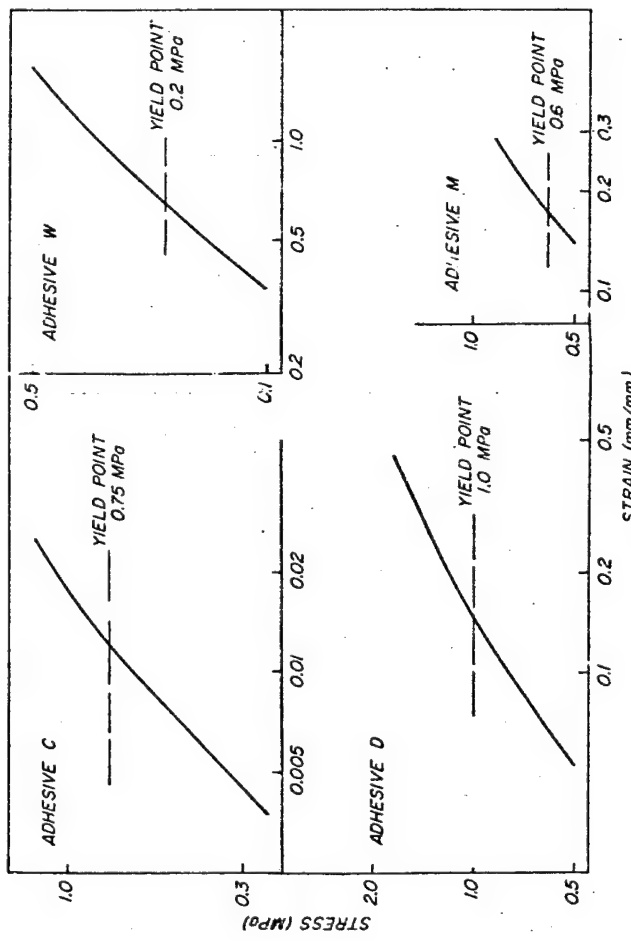


Figure 14.--Isochronous stress-strain curves showing the strain after 6 minutes at several constant stress levels.  
(M 146 250)

### Recovery Behavior

Turner (16) developed a simple graphic expression for the ability of a viscoelastic material to recover. Figure 15 shows the recovery behavior of adhesives M, D, and C expressed by this method. The vertical axis is the fraction of the creep strain recovered at a given time. The horizontal axis is the time allowed for the recovery as a percent of the total creep time.

The maximum recovery time in these experiments only equalled the creep time (reduced time = 1). Turner recommends that recovery should be allowed to continue for a period equal to the creep time (reduced time = 1) but, in most cases, reduced time need not exceed 4. Theoretically, the curves shown in figure 15 should extend upward to the right and approach a fractional recovery of 1 asymptotically at longer reduced times. However, it appears that reduced times of  $10^3$  or  $10^4$  would be necessary for complete recovery of adhesives D and C under these experimental conditions. Turner points out that the shape and extent of the curves will vary with the stress level and duration of creep. It is also possible these adhesives have suffered irrecoverable creep. Adhesive C, in particular, which appears to recover very slowly, also had a characteristically long delay time before reacting to the applied load under these load and environmental conditions.

Turner (16) describes how results of such recovery studies used in conjunction with standard creep data can be used to predict the course of recovery of a material after the removal of a given stress.

### Creep-Rupture Strength

The stress that will cause failure of a viscoelastic material decreases as the duration of load increases. The stress that causes failure at a given time is the creep-rupture strength. Some materials, such as crosslinked adhesives, may not fail within their service life if the stress is below a certain level. That level is the "endurance limit." Two methods, constant stress and constantly increasing stress, have been used to predict the endurance limit.

The constantly increasing stress or Prot method (10) tests successive specimens to failure at successively lower rates of loading. An equation fitted to the failure stress versus rate of load data is extrapolated to zero rate of load. The predicted stress at zero rate of load is the endurance limit. The Prot method has the advantages that each specimen contributes to the estimate of the endurance limit and the experimental time is short. As yet, no theory has been offered to explain this relationship. Nevertheless, Lewis, et al. (7) have found good agreement between endurance limits determined by the Prot and constant stress methods.

The constant stress method needs no justification. Its major disadvantages are long experimental times, and the fact that only the weakest specimens contribute toward defining the endurance limit at stress levels approaching the limit.

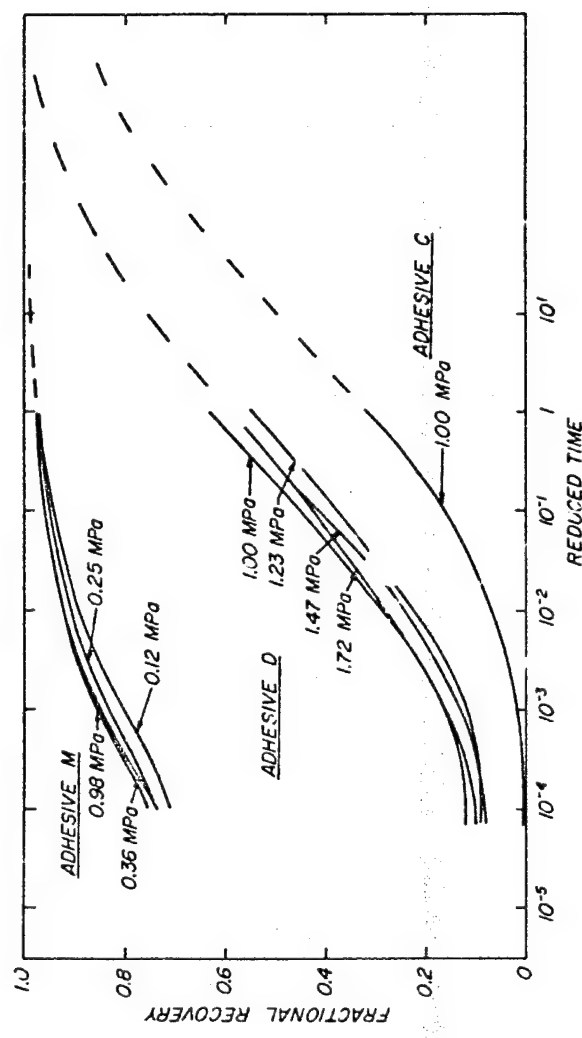


Figure 15.--Fractional recovery (fraction of total creep strain recovered) versus reduced time (recovery time expressed as a fraction of the time under load).  
(M 146 249)

The present creep test apparatus could be adapted to the Prot test by the addition of a shot loading or other mechanism for constantly increasing the stress. The apparatus can be used without modification for constant stress testing.

Sufficient numbers of specimens of adhesives D and W failed during the present long-term constant stress testing to illustrate the creep-rupture versus time relationship shown in figure 16. All adhesive W specimens loaded above the 0.1 MPa stress level failed so those data points represent five specimens. Adhesive D at all stress levels, and adhesive W at 0.1 MPa, had from two to three failures. Thus the failure times of these failures represent the average of the weaker specimens of the sample population. From figure 16, adhesive D appears to have an endurance limit near 1.0 MPa. Coincidentally, the isochronous stress-strain test of adhesive D indicated a yield stress of 1.0 MPa. Adhesive W does not appear to have an endurance limit on the basis of the limited data shown here.

#### Suggested Test Program

A standard method for conducting creep tests of adhesives in shear has not been developed. Excellent guidelines on procedure and data collection are outlined in ASTM D-2990 (1), and Thomas and Turner (17) provide a wonderfully detailed plan for creep testing. Their report is well worth reading for its discussion of creep test philosophy and equipment requirements as well as the detailed outline of a practical test procedure to determine any given visco-elastic relationship.

A program of tests condensed from these sources and based on environmental conditions common to wood structures should include the following:

1. Preliminary strength tests at 23° C - 44% RH, and 71° C - ambient RH, to help define the range of stress levels that will yield useful information in stress-strain and creep testing.
2. Preliminary low-load level short-term stress-strain tests of each creep test specimen at standard 23° C, 44% RH, to screen specimens and eliminate those with highly variable adhesive layers.
3. An abbreviated 6-minute stress-strain test of each specimen for the creep test at the creep stress test level. The data from this test can be used to check the accuracy of the creep test result.
4. Three to five creep tests on separate sets of specimens at various stress levels at each of the following conditions: 23° C, 44% RH; 50° C, 51% RH; and 70° C, 60% RH. To evaluate the effects of moisture, it is also desirable to conduct at least three creep-recovery tests at 23° C, 87% RH; 23° C, water soaked; and 50° C, 91% RH. The tests should extend to 4 months, including a recovery period at least as long as the time under load.
5. Two or more curves at 23° C, 44% RH, extending to 1 year and one curve for 3 years.

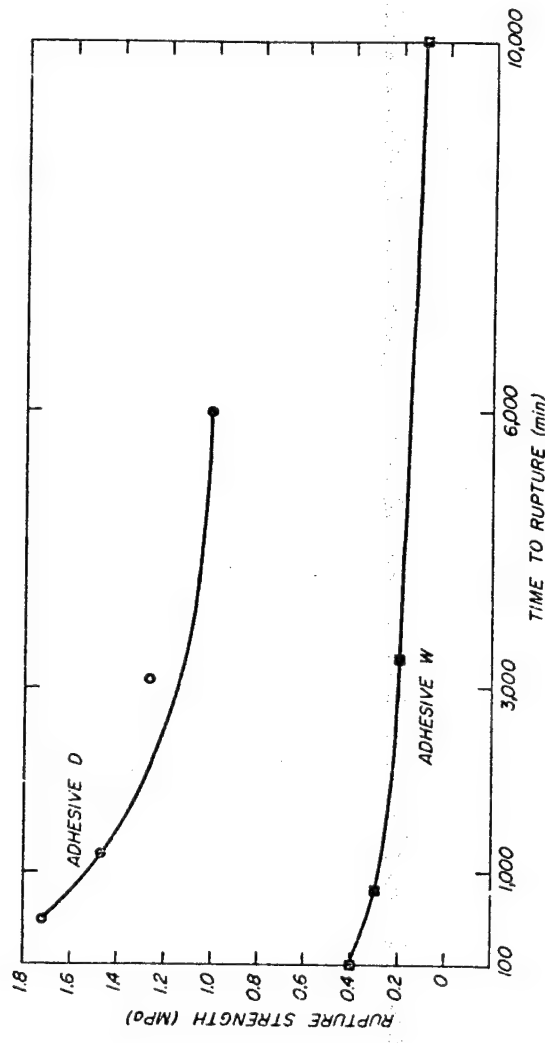


Figure 16.--Creep-rupture strength versus time, or the time to cause failure of weaker specimens at a given level of constant stress.  
(M 146 253)

Based on past experience (13) mastic construction adhesives generally will not withstand constant stress at useful design levels in the face of both maximum temperature and moisture 70° C, water soaked; therefore, while such conditions may occur in a structure, tests at these conditions are not warranted.

#### SUMMARY

A test apparatus was developed to evaluate the long-term stress-strain behavior of relatively flexible adhesives. The apparatus was designed for use in creep and creep-rupture testing, and to be easily convertible to stress-relaxation testing. Information useful to design engineers and adhesive formulators can be obtained with this apparatus. Preliminary tests revealed relationships between adhesive creep modulus and time, evidence of a yield point through isochronous stress-strain curves, trends in recovery behavior, and the creep-rupture strength of several mastic construction adhesives and a two-part polyurethane adhesive.

Not all the data obtained were useful. Many problems arose with failure of the electronic data collection system in the development stage. These failures were mainly related to manufacturing defects, however. The slip gage device for measuring adhesive slip should be redesigned to compensate for unwanted adherend movement or deformation. The data collection and temperature control systems, while operating satisfactorily, could be improved. These and other problems are discussed and suggestions were made for eliminating or minimizing them in future experiments.

## BIBLIOGRAPHY

1. American Society for Testing and Materials.  
1976. Standard method of test for tensile creep and creep rupture of plastics. ASTM D-2990, Part 35, Book of Standards.
2. American Society for Testing and Materials.  
1976. Standard definitions of terms relating to methods of mechanical testing, E-6, Part 35, Book of Standards.
3. Baier, E., J. R. Knox, T. J. Linton, and R. E. Maier.  
1960. Structural design of plastics. Society of Plastics Engineers Journal 16:396-406.
4. Goodman, J. R., and E. P. Popov.  
1968. Layered beam systems with interlayer slip. Journal of the Structural Division, ASCE, Vol. 94, No. ST11, Proc. Paper 6214, p. 2535-2547..
5. Kinney, G. F.  
1972. Creep data organized by a modulus equation. Modern Plastics. December. (See also Modern Plastics Encyclopedia 48(10A):602-621 for tabulation of creep modulus values for a wide variety of plastics.)
6. Kuenzi, E. W., and T. L. Wilkinson.  
1971. Composite beams--effect of adhesive or fastener rigidity. USDA For. Serv. Res. Pap. FPL 152.
7. Lewis, A. F., R. A. Kinmonth, and R. P. Kreahling.  
Long-term strength of structural adhesive joints. J. Adhesion 3:249-257.
8. McGee, W. D., and R. J. Hoyle.  
1974. Design method for elastomeric adhesive-bonded wood joist-deck systems. Wood and Fiber 6(2):144-155.
9. National Forest Products Association.  
1976. National design specification for stress-grade lumber and its fastenings. NFPA, Wash., D.C.
10. Prot, M. E.  
1948. Fatigue testing under progressive loading, a new technique for testing materials. Transl. WADC TR 52-148, by E. J. Ward.
11. Richards, J. A., R. P. Kerfoot, and G. P. Krueger.  
1975. Wood shear panels bonded with flexible adhesives. Jour. Struct. Div., Proc. ASCE, Vol. 1, ST 1, p. 131-149.
12. River, B. H.  
1973. Mastic construction adhesives in fire exposure. USDA For. Serv. Res. Pap. FPL 198.

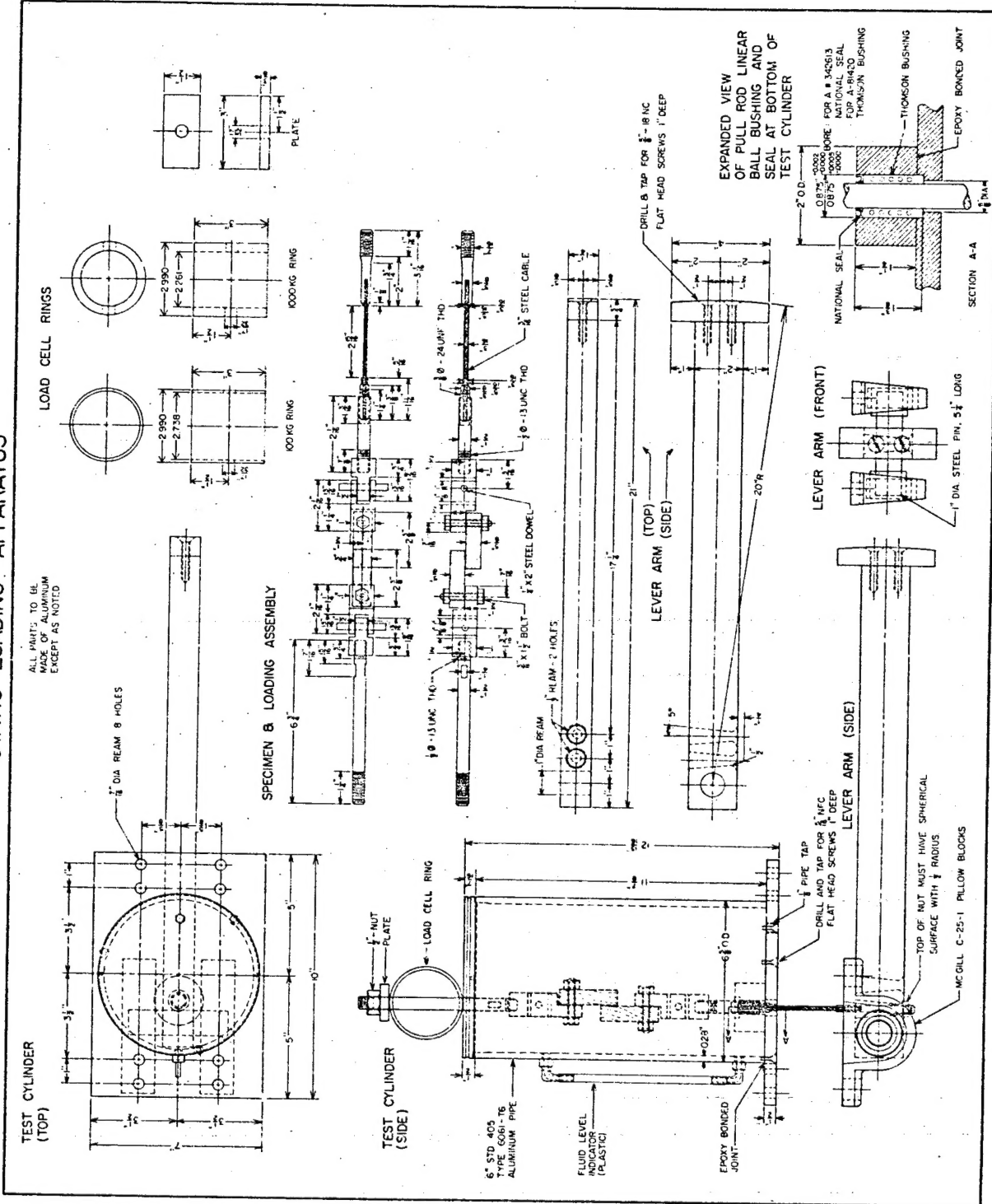
13. River, B. H.  
1978. Strength and shear modulus of several construction adhesives as influenced by environment and loading conditions. U.S. Department of Agriculture, Forest Service, Forest Products Laboratory report for Department of Housing and Urban Development, Office of Policy Development and Research.
14. River, B. H., and R. H. Gillespie.  
1978. Measurement of shear modulus and strength of adhesives. U.S. Department of Agriculture, Forest Service, Forest Products Laboratory report prepared for Department of Housing and Urban Development, Office of Policy Development and Research.
15. River, B. H., and R. H. Gillespie.  
Unpublished. A preliminary investigation of the behavior of elastomer-based mastic-type construction adhesives under long-term load.
16. Turner, S.  
1969. Deformation data for engineering design. Testing of Polymers, Vol. 4, Chap. 1. W. E. Brown, Ed. Intersci. Publ., N.Y.
17. Thomas, D. A., and S. Turner.  
1969. Experimental technique in uniaxial tensile creep testing. Testing of Polymers, Vol. 4, Chap. 2. W. E. Brown, Ed., Intersci. Publ., N.Y.

APPENDIX A

**Details of the Static Loading Apparatus**

## STATIC LOADING APPARATUS

ALL PARTS TO BE  
MADE OF ALUMINUM  
EXCEPT AS NOTED



## APPENDIX B

### Development of a Procedure to Calculate the Creep Shear Slip When Transducer Input Voltage is Variable

If the input voltage to the LVDT remained perfectly constant during the duration of the creep experiment, the core position at any time would be simply calculated by:

$$\Delta = \frac{1}{m_1} V_0 - a_1 \quad (\text{see fig. 7})$$

where:

$\Delta$  = core displacement,  
 $V_0$  = voltage output of the LVDT, and  
 $a_1, m_1$  = the regression constant and coefficient for  $V_0$  as a function of  $\Delta$ .

The core displacement and consequently the creep shear slip at any time (t) would be calculated by:

$$S = \Delta_o - \Delta_t = \frac{1}{m_1} \left[ V_{0_o} - V_{0_t} \right]$$

where:

$S$  = creep shear slip,  
 $\Delta_o - \Delta_t$  = core displacement between the time of initial loading (o) and some time (t).

But for various reasons the voltage supply to the LVDT is likely to vary or drift over the relatively long time periods of a creep test, and since LVDT output is a function of input voltage as well as the core position, it will vary with time and cause an error in the measured creep shear slip. This error can be minimized by calibrating the LVDT for input voltage,

$$V_0 = a_2 + m_2 V_I \quad (\text{see fig. 8})$$

where:

$V_I$  = voltage supplied to the LVDT,  
 $a_2, m_2$  = the regression constant and coefficient for  $V_0$  as a function of  $V_I$ .

Then establishing ( $m_2$ ) the change in the ratio  $V_o/V_I$  as a function of the core position:

$$m_2 = \frac{V_o - a_2}{V_I} = a_3 + m_3 \Delta \quad (\text{see fig. 8 inset})$$

it is possible to calculate  $\Delta$  for any input voltage regardless of core position

$$\Delta = \frac{1}{m_3} \left[ \frac{V_o}{V_I} - \frac{a_2}{V_I} - a_3 \right]$$

or the core displacement ( $\Delta_o - \Delta_t$ ) and creep shear slip ( $S$ ) can be calculated by

$$S = \Delta_o - \Delta_t = \frac{1}{m_3} \left[ \frac{V_{o_o}}{V_{I_o}} - \frac{a_2}{V_{I_o}} - a_3 \right] - \frac{1}{m_3} \left[ \frac{V_{o_t}}{V_{I_t}} - \frac{a_2}{V_{I_t}} - a_3 \right]$$

$$= \frac{1}{m_3} \left[ \frac{V_{o_o}}{V_{I_o}} - \frac{V_{o_t}}{V_{I_t}} + a_2 \left( \frac{1}{V_{I_t}} - \frac{1}{V_{I_o}} \right) \right]$$

But if  $a_2$  is assumed = to zero (actually experimental values of  $a_2$  ranged from 0 to 0.0053 with most values less than 0.0020) then the corrected creep shear slip may be simply calculated as

$$S = \frac{1}{m_3} \left[ L_o - L_t \right]$$

$L_o = V_{o_o}/V_{I_o}$  and  $m_3$  are constants. The ratio  $L_t = V_{o_t}/V_{I_t}$  is the test variable to be calculated in order to determine the corrected slip at any given time of the creep or recovery experiment.